Environment International 158 (2022) 106943

Contents lists available at ScienceDirect

Environment International

journal homepage: www.elsevier.com/locate/envint

Biotransformation of 2,4,6-tris(2,4,6-tribromophenoxy)-1,3,5-triazine (TTBP-TAZ) can contribute to high levels of 2,4,6-tribromophenol (2,4,6-TBP) in humans

Guomao Zheng [a], Luma Melo [b], Rishika Chakraborty [b], James E. Klaunig [b], Amina Salamova [a,*]

[a] Paul H. O'Neill School of Public and Environmental Affairs Indiana University, Bloomington, Indiana 47405, USA
[b] School of Public Health, Indiana University, Bloomington, Indiana 47405, USA

ARTICLE INFO

Handling Editor: Adrian Covaci

Keywords:
2,4,6-TBP
TTBP-TAZ
Biotransformation
In vitro
In vivo

ABSTRACT

2,4,6-Tribromophenol (2,4,6-TBP) is a brominated flame retardant that accumulates in human tissues and is a potential toxicant. Previous studies found 2,4,6-TBP levels in human tissues were significantly higher than those of brominated flame retardants measured in the same samples. In contrast, the levels of 2,4,6-TBP in the environment and foodstuff are not elevated, suggesting a low potential for direct intake through environmental exposure or diet. Here, we hypothesized that high levels of 2,4,6-TBP in human tissues are partially from the indirect exposure sources, such as biotransformation of highly brominated substances. We conducted *in vitro* assays utilizing human and rat liver microsomes to compare the biotransformation rates of four highly brominated flame retardants, which could potentially transform to 2,4,6-TBP, including decabromodiphenyl ethane (DBDPE), 2,4,6-tris-(2,4,6-tribromophenoxy)-1,3,5-triazine (TTBP-TAZ), 1,2-bis(2,4,6-tribromophenoxy)ethane (BTBPE), and tetrabromobisphenol A (TBBPA). Our results show that TTBP-TAZ rapidly metabolizes in both human and rat liver microsomes with a half-life of 1.1 and 2.2 h, respectively, suggesting that TTBP-TAZ is a potential precursor of 2,4,6-TBP. In contrast, 2,4,6-TBP was not formed as a result of biotransformation of TBBPA, BTBPE, and DBDPE in both human and rat liver microsomes. We applied suspect and target screening to explore the metabolic pathways of TTBP-TAZ and identified 2,4,6-TBP as a major metabolite of TTBP-TAZ accounting for 87% of all formed metabolites. These *in vitro* results were further tested by an *in vivo* experiment in which 2,4,6-TBP was detected in the rat blood and liver at concentrations of 270 ± 110 and 50 ± 14 μg/g lipid weight, respectively, after being exposed to 250 mg/kg body weight/day of TTBP-TAZ for a week. The hepatic mRNA expression demonstrated that TTBP-TAZ significantly activates the aryl hydrocarbon receptor (*AhR*) and promotes fatty degeneration (18 and 28-fold change compared to control, respectively) in rats.

1. Introduction

2,4,6-Tribromophenol (2,4,6-TBP) is used as a fungicide, wood preservative, and additive flame retardant in electronic products (Covaci et al., 2011; Koch and Sures, 2018). 2,4,6-TBP is a ubiquitous environmental contaminant that has been detected in soil, sludge, surface water, indoor dust and air, outdoor air, and landfill leachate (Koch and Sures, 2018). Exposure to 2,4,6-TBP has been associated with a range of toxic effects in *in vitro* and animal studies (Koch and Sures, 2018). 2,4,6-TBP is a strong endocrine disruptor acting through binding to transthyretin and inhibiting the thyroid sulfotransferase/deiodinase in human liver subcellular fractions and placenta cell line (Butt and Stapleton, 2013; Butt et al., 2011; Hamers et al., 2006; Leonetti et al., 2018). In addition, 2,4,6-TBP can disrupt the metabolic homeostasis by inhibiting recombinant UDP-glucuronosyltransferases, an important phase II drug-metabolizing enzyme (Wang et al., 2020). Exposure to 2,4,6-TBP exposure has been linked to neurological, reproductive, and developmental disorders in rats, zebrafish, and marine organisms (Deng et al., 2010; Hassenklöver et al., 2006; Lyubimov et al., 1998; Norman Haldén et al., 2010). There is limited information on the human health effects of exposure to 2,4,6-TBP; however, one recent study suggests that 2,4,6-TBP disrupts thyroid hormone regulation during pregnancy and affects neonatal development (Leonetti et al., 2016a).

Multiple studies have reported 2,4,6-TBP as an abundant brominated

* Corresponding author at: 702 N Walnut Grove Ave., Bloomington, IN 47405, USA.
E-mail address: asalamov@indiana.edu (A. Salamova).

https://doi.org/10.1016/j.envint.2021.106943
Received 13 August 2021; Received in revised form 24 September 2021; Accepted 13 October 2021
Available online 28 October 2021

compound in various human tissues, including blood, adipose, and placenta, detected at levels 10–100 times exceeding those of the ubiquitous polybrominated diphenyl ethers (PBDEs) measured in the same samples (Butt et al., 2016; Gao et al., 2015; Leonetti et al., 2016a; Leonetti et al., 2016b). Humans can be exposed to 2,4,6-TBP via various direct sources, such as dust ingestion, inhalation, dietary intake, and dermal contact (Gao et al., 2015; Guo et al., 2018; Takigami et al., 2009; Wang et al., 2011). However, the levels of 2,4,6-TBP in indoor dust (Guo et al., 2018), air (Guo et al., 2018), consumer products (Gao et al., 2015), and food (Wang et al., 2011) are significantly lower than those of other brominated flame retardants (BFRs), including PBDEs, suggesting that indirect sources could contribute to the accumulation of 2,4,6-TBP in humans.

Biotransformation of BFRs has been proposed as a potential indirect source of 2,4,6-TBP in humans (Gao et al., 2015). BDE-209 was suggested as a precursor of 2,4,6-TBP based on a significant correlation between the levels of BDE-209 and 2,4,6-TBP found in placenta (Leonetti et al., 2016b). However, several *in vitro* and *in vivo* metabolism studies did not observe a significant depletion of BDE-209 and formation of 2,4,6-TBP (Gao et al., 2015; Sandholm et al., 2003; Stapleton et al., 2008), suggesting that biotransformation of other brominated compounds structurally similar to BDE-209 could be a source of 2,4,6-TBP in humans. Previous studies have shown that some highly brominated flame retardants can degrade to 2,4,6-TBP in the environment. For example, 2,4,6-TBP has been identified as one of the thermal- and photodegradation products of 1,2-bis(2,4,6-tribromophenoxy)ethane (BTBPE) and tetrabromobisphenol A (TBBPA) (Barontini et al., 2004; Eriksson et al., 2004; Zhang et al., 2016). Moreover, 2,4,6-tris-(2,4,6-tribromophenoxy)-1,3,5-triazine (TTBP-TAZ) and decabromodiphenyl ethane (DBDPE) have been frequently detected in consumer products and dust along with 2,4,6-TBP (Ballesteros-Gómez et al., 2014; Schreder and Uding, 2019), suggesting common sources in the environment. These findings suggest that these four highly brominated compounds (TTBP-TAZ, TBBPA, DBDPE, and BTBPE) could be the precursors of 2,4,6-TBP. All four compounds are structurally similar to BDE-209 and have been widely used as replacements for the restricted octa-PBDEs and BDE-209, as well as for hexabromocyclododecane (Ballesteros-Gómez et al., 2014; Covaci et al., 2011). They have been detected at high concentrations in a range of consumer products and in the environment (e.g., indoor dust and air) and food (Guo et al., 2018; Xiong et al., 2019; Zuiderveen et al., 2020). However, few studies have focused on the biotransformation of these compounds in humans (Zalko et al., 2006).

In this study, we used an *in vitro* assay utilizing human and rat liver microsomes to examine whether the hepatic biotransformation of TTBP-TAZ, TBBPA, DBDPE, and BTBPE is a potential source of 2,4,6-TBP. The suspect and target screening approaches were applied to identify potential metabolites and their metabolic toxicity was further evaluated in an *in vivo* experiment.

2. Materials and methods

Chemicals and reagents. TTBP-TAZ, TBBPA, DBDPE and BTBPE were purchased from Toronto Research Chemicals. 2,4,6-Tribromoanisole was obtained from Sigma-Aldrich. A mixture of 19 bromophenols including 2-, 3-, 4-bromophenols, 2,3-, 2,4- 2,5-, 2,6-, 3,4-, 3,5-dibromophenols, 2,3,4-, 2,3,5-, 2,3,6-, 2,4,5-, 2,4,6-, 3,4,5-tribromophenols, 2,3,4,5-, 2,3,4,6-, 2,3,5,6-tetrabromophenols, and pentabromophenol, was obtained from Wellington Laboratories. All solvents used in this study were Optima grade. Mixed gender human liver microsomes (pool size = 50) and mixed gender Sprague-Dawley rat liver microsomes (pool size = 50) were obtained from Sekisui XenoTech and Bioivt, respectively, and the NADPH regeneration system was from Promega.

In vitro microsomal incubations. Incubations were performed with human and rat liver microsomes separately in 1.5 mL amber glass vials at 37 °C using previously published methods (Ashrap et al., 2017; Gao et al., 2015). Briefly, a 200 μL reaction mixture containing 50 mM phosphate buffer (pH 7.4) with 3 mM $MgCl_2$, liver microsomes at a final concentration of 1 mg/mL, and a 0.1–5 μM substrate (final concentration) was delivered in 1 μL of acetone. Reactions were initiated by the addition of a NADPH regeneration system (NADP 6.5 mM, glucose 6-phosphate 16.5 mM, $MgCl_2$ 16.5 mM, and glucose 6-phosphate dehydrogenase 2 U/mL) and were performed in triplicates at 37 ^{0}C. After 2 h, 200 μL of chilled acetone was added to terminate the reaction. Negative control samples were prepared with heat-deactivated microsomes to assess potential background interferences and non-enzymatic changes. After the incubation, the mixture was spiked with surrogate standards (BDE-77 and $^{13}C_{12}$-BDE-209), liquid–liquid extracted with 2 mL hexane twice and then with 2 mL 1:1 hexane/dichloromethane (v/v). The combined extracts were concentrated to dryness using nitrogen, reconstituted in 1 mL hexane and spiked with internal standards (BDE-118 and -181) for instrumental analyses.

Animal experiments. Male 4 weeks old Sprague-Dawley rats ($n = 15$) were purchased from Taconic Biosciences and housed (three per cage) under controlled temperature (22 ± 1 °C), humidity (40–70%), and light cycle (12 h/12 h) with ad libitum food and water. All rats were quarantined for 7 days prior to the initiation of the study, and then assigned randomly into the control group ($n = 5$), 250 mg/kg body weight (bw)/day TTBP-TAZ exposure group ($n = 5$), or 250 mg/kg bw/day 2,4,6-TBP exposure group ($n = 5$). Both TTBP-TAZ and 2,4,6-TBP were diluted in corn oil and the control group received corn oil. The administration was done orally by gavage for 7 days. In the sacrifice, liver, thyroid, and blood were collected. Initial and final body weights along with liver and thyroid weights at terminal sacrifice were measured. Blood samples were allowed to clot at room temperature for 30 min, and then centrifuged at 3000 rpm for 15 min to separate serum. Animals were housed in the Indiana University AAALAC-certified animal facility and maintained according to the Guide for the Care and Use of Laboratory Animals from the Institute of Laboratory Animal Research under a protocol approved previously by the Institutional Animal Care and Use Committee at Indiana University.

Sample treatment. 0.1 g of the sample (either rat serum or liver) was homogenized with 1 mL of 1% potassium chloride and then spiked with the surrogate standards (BDE-77 and $^{13}C_{12}$-BDE-209). Hydrochloric acid (6 M, 0.5 mL) and 3 mL isopropanol were added to denaturize the samples. Samples were further extracted with 3 mL of a 1:1 hexane/methyl *tert*-butyl ether mixture (v/v) three times and the supernatants were combined. The lipid content was determined gravimetrically using 10% of the combined extract. The rest of the extract was then concentrated to dryness using nitrogen, reconstituted in 1 mL hexane and spiked with internal standards (BDE-118 and -181).

Instrumental analyses. The full scan mass spectra (suspect screening) of the samples from the dose experiments and the 2,4,6-TBP standard were analyzed on an Agilent 6890 gas chromatograph (GC) coupled to an Agilent 5973 mass spectrometer (MS) in the electron ionization (EI) mode (70 V electron energy). Chromatographic separation was achieved with an Rtx1614 column (30 m, 250 μm i.d., 0.1 μm film thickness) at a flow rate of 1 mL/min. The oven temperature was programmed as follows: 80 °C for 5 min, increased to 220 °C at 10 °C/min, held at 220 °C for 1 min, increased to 300 °C at 30 °C/min, and held at 300 °C for 6 min. High purity helium (99.999%; Indiana Oxygen) was used as the carrier gas. The GC/MS transfer line was maintained at 300 °C. The temperature of the ion source and quadrupole mass analyzer was set at 230 °C and 150 °C, respectively. One μL of the sample was injected in the pulsed spitless mode at 250 °C. The analysis was performed in a full scan mode in the mass range of m/z 50 to m/z 800.

Twenty-four target compounds including TTBP-TAZ, TBBPA, DBDPE, BTBPE, 2,4,6-tribromoanisole and 19 bromophenols (target screening) were analyzed on an Agilent 7890 GC coupled to an Agilent 5977B MS in the electron capture negative ionization (ECNI) mode. The mass spectrometer ion source and quadrupole temperatures were maintained at 200 and 106 °C, respectively. Two μL was injected in the pulsed spitless mode at 240 °C. Chromatographic resolution was

achieved with an Rtx1614 (15 m, 250 μm i.d., 0.1 μm film thickness) fused silica capillary GC column (Restek Corporation). The carrier gas was helium (99.999%; Liquid Carbonic) regulated at a constant flow of 1.5 mL/min. The GC oven temperature was programmed as follows: 100 °C for 2 min, 25 °C/min to 250 °C, 3 °C/min to 270 °C, 25 °C/min to 300 °C, and 300 °C for 6 min. The GC/MS transfer line was maintained at 280 °C. Selected ion monitoring of *m/z* 79 and 81 was used to quantitate most of the target compounds. TTBP-TAZ and $^{13}C_{12}$-BDE209 were monitored at *m/z* 751.7/753.7 and 494.6/496.6, respectively.

mRNA expression. Quantitative real-time PCR was used to determine the expression of mRNA levels of genes related to inflammation (*INFγ, TNFα, IL-6*), oxidative stress (*HOMX1, AOX1, SOD1, CAT*), angiogenesis (*VEGF, MYC, HIF1α*), liver metabolism (*ANGPTL4, PLIN, LPL*), liver nuclear receptors (*CAR, RXRα, RXRβ, RXRγ, PPARα, PPARγ, PPARδ, FXR, LXR, PXR, AhR*), and thyroid genes in liver tissue (*TG, THRβ, TSH*). The β2 microglobulin (*B2m*) was used as an internal control for data normalization. The primers for these genes are listed in Table S1. The relative expression level of mRNA for each gene was calculated by method $2^{-\Delta\Delta Ct}$ (Livak and Schmittgen, 2001).

Data analysis. Full-scan MS^1 spectra of the dosed and control samples obtained from GC-MS (EI) were converted to mzXML format and introduced into the XCMS platform (http://xcmsonline.scripps.edu) for feature detection. The datasets were pre-processed by performing peak detection, filtering, and alignment. Thereafter, normalized peak area matrices (a total of 655 features) were exported to MetaboAnalyst (http://www.metaboanalyst.ca) for multivariate statistical analysis. Clustering of the samples was assessed using principal component analysis (PCA) to reveal the differences between the dosed and control samples. Orthogonal partial least-squares-discriminant analysis (OPLS-DA) was carried out to generate the maximum separation between the groups of dosed and control samples.

In vitro biotransformation rates (CL_{int}, mL/h/mg) were determined based on a Lineweaver-Burk plot using Equations (1) and (2) (Greaves et al., 2016) and half-lives ($t_{1/2}$, h) were calculated using Equation (3)

$$\frac{1}{V} = \frac{K_m}{V_{max}} \times \frac{1}{[S]} + \frac{1}{V_{max}} \quad (1)$$

$$CL_{int} = \frac{V_{max}}{K_m} \quad (2)$$

$$t_{1/2} = \frac{Ln(2)}{CL_{int}} \times C_{protein} \quad (3)$$

where V_{max} was the maximum biotransformation rate for a saturated system (nmol/h/mg), K_m was the Michaelis constant representing the substrate concentration at one half of the V_{max} (μM or nmol/mL), V was the biotransformation rate of substrates (nmol/h/mg), [S] was the substrate concentration (μM or nmol/mL), $C_{protein}$ was the protein concentration (mg/mL) of the incubation mixtures.

Descriptive statistics were calculated using IBM SPSS Statistics 24 and Microsoft Excel 2016, and plots were generated using Sigma Plot 13 (Systat Software Inc.). A *p* value of 0.05 was used to define significance.

Quality assurance and quality control. All glassware used in these experiments was muffled at 500 °C for 6 h before use. Procedural blanks were analyzed with every batch of 6 samples to monitor background contamination. Method detection limits (MDLs) were set at three times the standard deviation of the target analyte levels detected in blanks. For compounds not detected in blanks, MDLs were based on a signal-to-noise ratio of three. The reported concentrations were blank-corrected by subtracting the average blank concentrations for each target compound from the sample levels. The absolute recoveries for the spiked samples were 77 to 110% for target compounds. The recoveries of the surrogate standards (mean ± standard error) were 108 ± 4.8 and 117 ± 5.0% for BDE-77 and $^{13}C_{12}$-BDE-209, respectively. The reported data were corrected based on the percent recoveries of the surrogate standards.

3. Results and discussion

In vitro biotransformation. In vitro biotransformation rates of TTBP-TAZ, TBBPA, DBDPE and BTBPE incubated with human and rat liver microsomes are summarized in Table 1. The results of these experiments fitted the Lineweaver-Burk curve for all four compounds (Figure S1, $R^2 > 0.921$). The highest hepatic biotransformation rate was observed for TTBP-TAZ (0.62 mL/h/mg), followed by BTBPE (0.10 mL/h/mg), TBBPA (0.08 mL/h/mg), and DBDPE (0.08 mL/h/mg). A similar trend was observed in the rat hepatic biotransformation experiment: TTBP-TAZ was metabolized faster than the other 3 compounds (0.32 mL/h/mg), but slower than in the human liver microsomes. The slow biotransformation of DBDPE, BTBPE, and TBBPA in both human and rat hepatic microsomes was consistent with the previous *in vitro* studies for PBDEs (Gao et al., 2015; Lupton et al., 2009; Stapleton et al., 2008). For example, BDE-47, BDE-153, and BDE-209 were resistant to metabolism in human liver microsomes with *in vitro* biotransformation rates of 0.09 to 0.141 mL/h/mg (Gao et al., 2015), which were similar to those found for TBBPA, BTBPE, and DBDPE in this study. Interestingly, the biotransformation rate of TBBPA determined using rat liver microsomes (0.23 mL/h/mg) was twice as high as that estimated using human liver microsomes, but no significant differences were found for BTBPE and DBDPE. The relatively fast biotransformation of TBBPA in rat liver microsomes is consistent with previous research and possibly related to differences in enzymatic activities of cytochrome P450 (Zalko et al., 2006).

Overall, our results show that TTBP-TAZ is rapidly metabolized in both human and rat liver microsomes with a half-life of 1.1 and 2.2 h, respectively. These half-lives are consistent with the half-life of TTBP-TAZ determined under direct photolysis (Lörchner et al., 2019).

Metabolic pathways of TTBP-TAZ biotransformation. Although TTBP-TAZ has been suggested as a precursor of 2,4,6-TBP in the environment (Koch and Sures, 2018; Lörchner et al., 2019), there is no evidence showing that TTBP-TAZ can be transformed to 2,4,6-TBP in the human body. Previous studies have reported that only debromination products were detected in photodegradation or electrochemical conversion of TTBP-TAZ (Lörchner et al., 2019; Lörchner et al., 2018). Here, suspect and target screening strategies were applied to explore the metabolic pathways of TTBP-TAZ biotransformation and to identify potential metabolites. First, extracts from the control and TTBP-TAZ human liver microsome incubations were analyzed using a suspect screening approach. The spectral data of all samples were analyzed using PCA. Figure S2A shows the PCA results where each point in the score plots represents an individual sample and samples with similar variances are grouped together. The control group and the three dosed groups (TTBP-TAZ at 1, 2.5, and 5 μM) showed a distinct separation, indicating that the biotransformation of TTBP-TAZ resulted in a significantly different metabolic profile. The S plots of the OPLS-DA model of the dosed and control groups datasets were used to extract the discriminatory metabolites that were responsible for class separation (Figure S2B). A

Table 1
In vitro intrinsic clearance rates (CL_{int}, mL/h/mg) of TTBP-TAZ, TBBPA, BTBPE, and DBDPE and their respective 2,4,6-TBP formation rates (mL/h/mg) in human and rat liver microsomes. Biotransformation of TBBPA, BTBPE, and DBDPE did not yield 2,4,6 TBP in both human and rat microsomes; hence formation rates were not calculated for these compounds.

	Human liver microsomes	Rat liver microsomes
Depletion		
TTBP-TAZ	0.62	0.32
TBBPA	0.08	0.23
BTBPE	0.10	0.14
DBDPE	0.08	0.09
Formation of 2,4,6-TBP		
TTBP-TAZ	1.34	0.77

discriminatory metabolite yielded the mass spectrum of Metabolite 1 (M1) at a retention time of 16.0 min (Fig. 1A) and based on the presence of the molecular ion at *m/z* 329.7 ($[M]^+$) and MS/MS fragment ion of 249.8 ($[M-Br]^+$) was deduced to result from 2,4,6-TBP. The structure of this discriminatory metabolite was further confirmed with a commercially available standard of 2,4,6-TBP where its retention time and mass spectrum matched well with those of the compound formed as a result of biotransformation (Fig. 1B), indicating that hepatic metabolism of TTBP-TAZ generated 2,4,6-TBP. Trace amounts of 2,4,6-TBP were found in the control group and can be explained by the impurities in the commercial standard of TTBP-TAZ. This was further confirmed by the mass spectrum of the TTBP-TAZ standard and the *in vitro* control samples in which 2,4,6-TBP accounted for 0.1% (v/v). Hydroxylated TTBP-TAZ metabolites were putative Phase I metabolites of TTBP-TAZ from the BioTransformer (http://biotransformer.ca/) but were not identified in this study, suggesting oxidation is not a major pathway for TTBP-TAZ hepatic metabolism.

The proposed metabolic pathways of TTBP-TAZ biotransformation are summarized in Fig. 2. Possible hydrolysis, isomeric, methylation, and debromination metabolites of TTBP-TAZ were identified using target screening. 2,4,6-TBP was the most abundant metabolite, accounting for 87% of the total TTBP-TAZ metabolite concentrations. The mechanism proposed for the hydroxylation pathway involves the OH radical attacking the carbon–oxygen bond, similar to the mechanism proposed for BDE-99 in previous *in vitro* and *in vivo* metabolism studies (Qiu et al., 2007; Stapleton et al., 2008). 2,4,5-Tribromophenol (2,4,5-TBP) was identified as the isomer of 2,4,6-TBP but at relatively low levels (12.6%). The formation of 2,4,5-TBP can be explained by a 1,2-shift of bromine via arene oxide intermediate, which has been reported as the formation mechanism of hydroxylated metabolites in the biotransformation of BDE-47 in rats and plants (Qiu et al., 2007; Sun et al., 2013). Interestingly, the concentration ratio of 2,4,6-TBP to 2,4,5-TBP was 6.9, which was consistent with that reported for human blood (6.5) (Qiu et al., 2009), further suggesting that TTBP-TAZ can be a significant source of 2,4,6-TBP in humans. Although methylation is a common metabolic pathway for most phenolic contaminants (e.g., hydroxylated PBDEs, triclosan, and TBBPA) in aquatic organisms and plants (Balmer et al., 2004; Hou et al., 2018; Leiker et al., 2009; Sun et al., 2016), 2,4,6-tribromoanisole (2,4,6-TBA), a possible product of TTBP-TAZ methylation, was detected at low levels (0.02%), probably due to the differences in enzymatic activities in humans. The only detectable debromination metabolites were 2,4-dibromophenol (2,4-DBP) (0.19%) and 4-bromophenol (0.19%), indicating debromination of 2,4,6-TBP at the *ortho* position, possibly due to reduction of steric hindrance (Stapleton et al., 2004; Zhang et al., 2019). The selective debromination of 2,4,6-TBP to 2,4-DBP was also reported in plants (Zhang et al., 2019). Although conjugation metabolites of TTBP-TAZ were not identified in this study, TBP-glucuronide and TBP-sulfate are the expected metabolites formed in this process (Ho et al., 2015).

2,4,6-TBP was formed rapidly as a result of human and rat hepatic

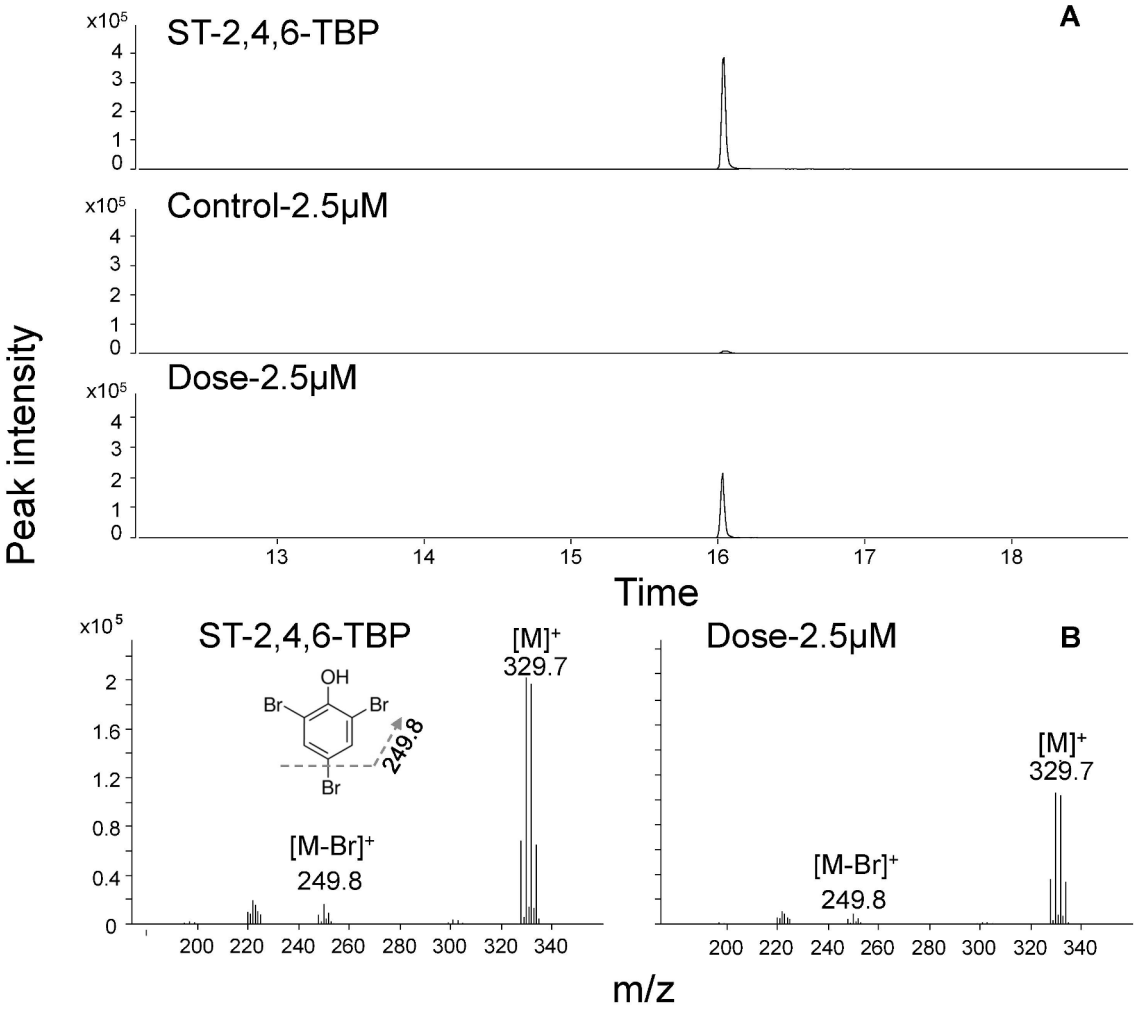

Fig. 1. The extracted chromatograms of *m/z* 329.7 for the 2,4,6-TBP standard (ST-2,4,6-TBP), a control sample, and a dosed sample isolated from TTBP-TAZ incubations (A); the mass spectra and proposed structures of the metabolite in the 2,4,6-TBP standard and in the dosed sample (B).

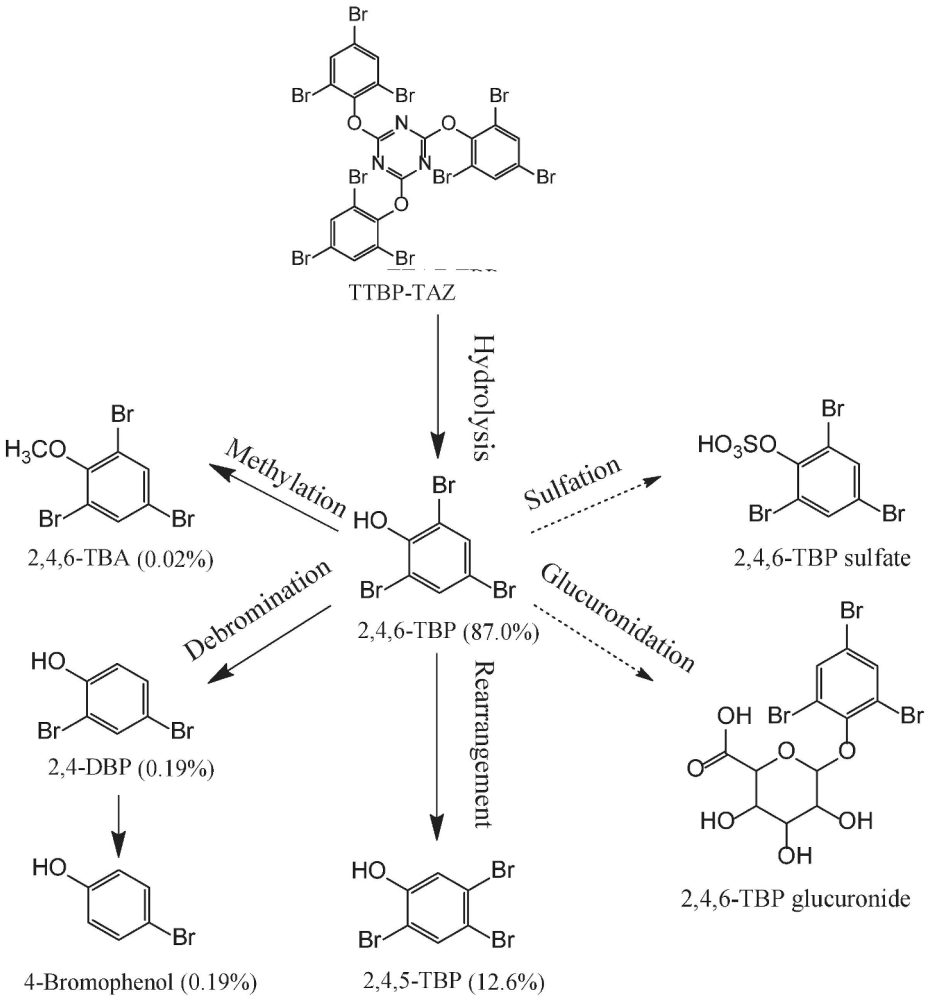

Fig. 2. Proposed pathways of the TTBP-TAZ hepatic biotransformation. Solid arrows indicate pathways determined in this study and dashed arrows indicate pathways reported in (Ho et al., 2015).

metabolism (at rates of 1.34 and 0.77 mL/h/mg, respectively) with the metabolite / parent (M/P) ratios of 2.16 and 2.40 (2,4,6-TBP to TTBP-TAZ), respectively, indicating that TTBP-TAZ is almost completely metabolized (a theoretical M/P of 3 is expected based on the chemical structure of TTBP-TAZ). The rapid *in vitro* formation rate of 2,4,6-TBP indicates that exposure to TTBP-TAZ can be a significant indirect source of 2,4,6-TBP in humans. In contrast, 2,4,6-TBP was not formed as a result of biotransformation of TBBPA, BTBPE, and DBDPE in both human and rat liver microsomes.

TTBP-TAZ and 2,4,6-TBP occurrence in exposed rats. The above results demonstrate the biotransformationof TTBP-TAZ in an *in vitro* system. We further tested whether 2,4,6-TBP could be formed in an *in vivo* experiment in which rats were exposed to TTBP-TAZ through gavage. Consistent with the results of the *in vitro* experiment, 2,4,6-TBP was detected in the rat blood and liver at concentrations of 270 ± 110 and 50 ± 14 μg/g lipid weight (lw), respectively, after being exposed to 250 mg/kg bw/day TTBP-TAZ for a week (Fig. 3). At the same time, no TTBP-TAZ was detected in any blood or liver samples. These results suggest that TTBP-TAZ can be metabolized quickly in rat liver after oral administration and its main metabolite, 2,4,6-TBP, can be transferred to blood. Furthermore, high concentrations of 2,4,6-TBP were detected in blood (460 ± 84 μg/g lw) and liver (2100 ± 900 μg/g lw) when rats were exposed to the same amount of 2,4,6-TBP. The average formation rate of 2,4,6-TBP was 5.7% and 1.3% in blood of rats exposed to 2,4,6-TBP and TTBP-TAZ, respectively. This rate increased to 14% in the liver of the rats exposed to 2,4,6-TBP, but decreased to 0.6% in rats exposed to

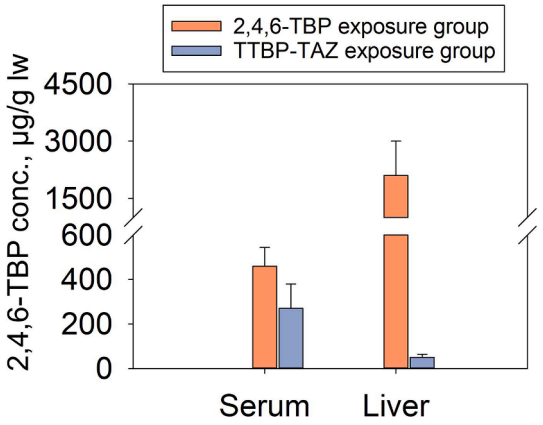

Fig. 3. Concentrations of 2,4,6-TBP in rat serum and liver (μg/g lw) of the 2,4,6-TBP exposure and TTBP-TAZ exposure groups (mean ± standard errors; n = 5). The control group is not shown because 2,4,6-TBP was not detected in this group.

TTBP-TAZ. The relatively low formation rate of 2,4,6-TBP in rats exposed to TTBP-TAZ can be explained by other factors, such as absorption efficiency, distribution, and elimination processes (Hakk and Letcher, 2003). For example, only 10% of DBDPE, a highly brominated compound, was absorbed in animal studies and 90% was excreted in

feces (Mörck et al., 2003).

mRNA expression. To investigate whether 2,4,6-TBP and TTBP-TAZ disrupt the liver and thyroid functions, we measured the mRNA expression levels of biomarker genes associated with nuclear receptors, oxidative stress, angiogenesis, inflammation, and lipid metabolism in the target tissue from the rats exposed to 2,4,6-TBP and TTBP-TAZ (Fig. 4). No significant difference was found for the relative body, liver, and thyroid weights (Table S2).

In this study, *TSH* was significantly induced in both TTBP-TAZ and 2,4,6-TBP exposed groups (Fig. 4). However, *THRβ* was significantly inhibited in the 2,4,6-TBP group, along with *TG* inhibition in the TTBP-TAZ group. From all the nuclear receptor genes tested (Table S1), *RXRα, RXRβ, RXRγ, PPARδ, PPARγ, LXR*, and *PXR* were significantly downregulated after exposure to 2,4,6-TBP, and *RXRα, RXRβ, RXRγ, and PXR* were significantly downregulated after exposure to TTBP-TAZ. However, and most interestingly, *AhR* was induced with 18-fold change after exposure to TTBP-TAZ when compared to control. All oxidative stress related genes (*HOMX1, AOX1, SOD1, CAT*) were significantly inhibited by the exposure to TTBP-TAZ, and *HOMX1, SOD1*, and *CAT* by the exposure to 2,4,6-TBP when compared to control. As for the angiogenesis related genes, *VEGF* and *HIF1α* were significantly inhibited for both treatment groups when compared to control, and *MYC* was significantly induced when compared to the 2,4,6-TBP exposure group. Regarding the inflammation genes, *INFγ, TNFα*, and *IL-6* were significantly decreased after 2,4,6-TBP treatment, and *INFγ* and *TNFα* were significantly reduced after TTBP-TAZ exposure. For lipid metabolism related genes, *PLIN* (28-fold change for TTBP-TAZ and 2.4-fold for 2,4,6 TBP) was the only significantly induced gene, while *ANGPTL4* and *LPL* were significantly inhibited.

Considering *AhR* is primarily responsible for the transcriptional regulation of CYP1A enzymes (Monostory et al., 2009), the significant induction of *AhR* in liver of the rats exposed to TTBP-TAZ suggests CYP1A may be involved in the hepatic metabolism of TTBP-TAZ. Moreover, the activation of *AhR* by TTBP-TAZ will enhance the metabolic toxicity of coexisting environmental contaminants, such as polycyclic aromatic hydrocarbons, which are known to generate an active *o*-semiquinone anion radical under the catalysis by CYP1A enzymes (Luo et al., 2019). Previous *in vitro* studies have demonstrated photolytic degradation products of tetradecabromo-1,4-diphenoxybenzene and BDE-209 (e.g., polybrominated dibenzofurans) can significantly upregulate mRNA expression of *AhR*-mediated CYP1A4 (Su et al., 2014; Su et al., 2016; Su et al., 2018). In the current study, however, it is unclear if the mRNA expression of *AhR* is induced by TTBP-TAZ or its metabolites, such as 2,4,6-TBP or other potential metabolites.

In addition, the downregulation of genes associated with oxidative stress (*HMOX1, SOD1*, and *CAT*) in both treatment groups suggests TTBP-TAZ has the same potential as 2,4,6-TBP to promote tumorigenesis (Li et al., 2019). Similarly, the downregulation of *HIF1α* found in both treatments was previously related to tissue regeneration in adult mice (Zhang et al., 2015) that could be linked to the reduction of *IFN-γ* expression known to increase the infiltration of activated T cells (Matsubara et al., 1999) and attenuate hepatic inflammation and fibrosis (Luo et al., 2013). Our results also demonstrated that the exposure to 2,4,6-TBP and TTBP-TAZ downregulated *VEGF* which was previously shown to cause impairment of lipoprotein uptake and reduction of hepatocellular lipid content (Carpenter et al., 2005). The latter two are in accordance with the inhibition of *ANGPTL4* and *LPL* found in both treatment groups (Bergö et al., 2002; Yamada et al., 2006). Specifically, *PLIN* was significantly induced in the TTBP-TAZ exposure group, being an indicator of undergoing fatty degeneration (Zhang et al., 2018).

Taken together, TTBP-TAZ can disrupt thyroid hormone homeostasis, nuclear receptors, oxidative stress, angiogenesis, inflammation, and lipid metabolism at the same exposure level as 2,4,6-TBP. To the best of our knowledge, this is the first study to examine the toxicity directly

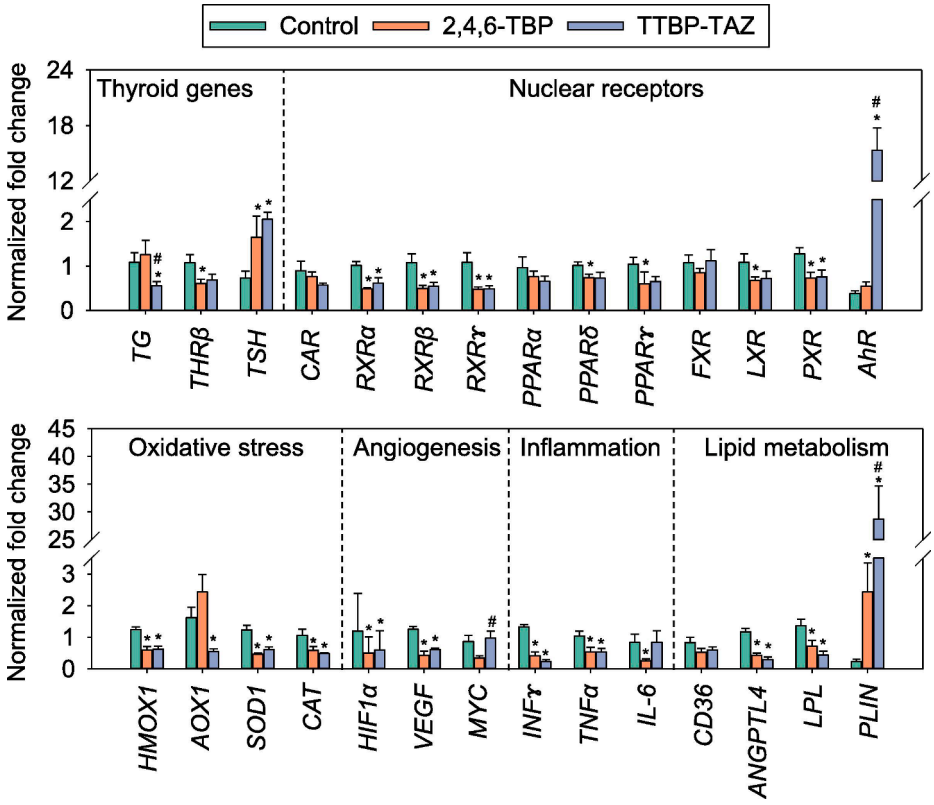

Fig. 4. mRNA expression (mean ± standard errors; $n = 5$) of genes encoding for thyroid functions, nuclear receptors, oxidative stress, angiogenesis, inflammation, and lipid metabolism in rat livers of the control group, 2,4,6-TBP exposure group, and TTBP-TAZ exposure group. * indicates a statistical difference from control and # indicates a statistical difference from 2,4,6 TBP at $p < 0.05$ (determined using ANOVA followed by Dunnett's post-hoc test).

associated with TTBP-TAZ.

In conclusion, this study has identified 2,4,6-TBP as the main hepatic biotransformation product of TTBP-TAZ in *in vitro* and *in vivo* experiments. Our results may provide an explanation for the findings of Gao et al. (2015), Leonetti et al. (2016b), and Butt et al. (2016) that reported significantly higher concentrations of 2,4,6-TBP compared to the other BFRs measured in human tissues (Butt et al., 2016; Gao et al., 2015; Leonetti et al., 2016b). The use of TTBP-TAZ has increased over the past years as it has been used as a replacement for PBDEs (Ballesteros-Gómez et al., 2014; Guo et al., 2018). European Chemicals Agency has listed TTBP-TAZ as a high production volume chemical (1000–10,000 tons per year) in 2019 (Zuiderveen et al., 2020). A recent report determined TTBP-TAZ as the most abundant flame retardant in six brands of television, constituting 3.5–12% of the product's weight (Schreder and Uding, 2019). In addition, previous studies showed TTBP-TAZ was frequently detected in a range of consumer products, air, and house dust, demonstrating widespread environmental exposure (Ballesteros-Gómez et al., 2014; Guo et al., 2018; Hammel et al., 2018; Stubbings et al., 2019). Considering the prevalent occurrence of TTBP-TAZ in the environment and consumer products, its significant contribution to the formation of 2,4,6-TBP in humans, and the strong endocrine disrupting potential of 2,4,6-TBP, our findings warrant further research on TTBP-TAZ toxicity.

Credit authorship contribution statement

Guomao Zheng: Conceptualization, Laboratory and Data analysis, Writing – original draft. **Luma Melo:** Conceptualization, Laboratory and Data analysis, Writing – review & editing. **Rishika Chakraborty:** Laboratory analysis. **James E. Klaunig:** Supervision, Conceptualization. **Amina Salamova:** Supervision, Conceptualization, Writing – review & editing.

Declaration of Competing Interest

The authors declare that they have no known competing financial interests or personal relationships that could have appeared to influence the work reported in this paper.

Acknowledgements

We thank Drs. Chen Wang and Staci Capozzi for their helpful feedback on this manuscript. G. Zheng and A. Salamova were supported by National Institute of Environmental Health Science R01 2R01ES019620-06A1.

Appendix A. Supplementary data

Supplementary data to this article can be found online at https://doi.org/10.1016/j.envint.2021.106943.

References

Ashrap, P., Zheng, G., Wan, Y., Li, T., Hu, W., Li, W., Zhang, H., Zhang, Z., Hu, J., Li, W., Wan, Y., Hu, W., Ashrap, P., Zhang, H., Zheng, G., Hu, J., Li, T., 2017. Discovery of a widespread metabolic pathway within and among phenolic xenobiotics. Proc. Natl. Acad. Sci. U. S. A. 114, 6062–6067.

Ballesteros-Gómez, A., De Boer, J., Leonards, P.E.G., 2014. A novel brominated triazine-based flame retardant (TTBP-TAZ) in plastic consumer products and indoor dust. Environ. Sci. Technol. 48, 4468–4474.

Balmer, M.E., Poiger, T., Droz, C., Romanin, K., Bergqvist, P.-A., Müller, M.D., Buser, H.-R., 2004. Occurrence of methyl triclosan, a transformation product of the bactericide triclosan, in fish from various lakes in Switzerland. Environ. Sci. Technol. 38, 390–395.

Barontini, F., Marsanich, K., Petarca, L., Cozzani, V., 2004. The thermal degradation process of tetrabromobisphenol A. Ind. Eng. Chem. Res. 43, 1952–1961.

Bergö, M., Wu, G., Ruge, T., Olivecrona, T., 2002. Down-regulation of adipose tissue lipoprotein lipase during fasting requires that a gene, separate from the lipase gene, is switched on*. J. Biol. Chem. 277, 11927–11932.

Butt, C.M., Miranda, M.L., Stapleton, H.M., 2016. Development of an analytical method to quantify PBDEs, OH-BDEs, HBCDs, 2,4,6-TBP, EH-TBB, and BEH-TEBP in human serum. Anal. Bioanal. Chem. 408, 2449–2459.

Butt, C.M., Stapleton, H.M., 2013. Inhibition of thyroid hormone sulfotransferase activity by brominated flame retardants and halogenated phenolics. Chem. Res. Toxicol. 26, 1692–1702.

Butt, C.M., Wang, D., Stapleton, H.M., 2011. Halogenated phenolic contaminants inhibit the in vitro activity of the thyroid-regulating deiodinases in human liver. Toxicol. Sci. 124, 339–347.

Carpenter, B., Lin, Y., Stoll, S., Raffai, R.L., McCuskey, R., Wang, R., 2005. VEGF is crucial for the hepatic vascular development required for lipoprotein uptake. Development 132, 3293.

Covaci, A., Harrad, S., Abdallah, M.A.E., Ali, N., Law, R.J., Herzke, D., de Wit, C.A., 2011. Novel brominated flame retardants: A review of their analysis, environmental fate and behaviour. Environ. Int. 37, 532–556.

Deng, J., Liu, C., Yu, L., Zhou, B., 2010. Chronic exposure to environmental levels of tribromophenol impairs zebrafish reproduction. Toxicol. Appl. Pharmacol. 243, 87–95.

Eriksson, J., Rahm, S., Green, N., Bergman, Å., Jakobsson, E., 2004. Photochemical transformations of tetrabromobisphenol A and related phenols in water. Chemosphere 54, 117–126.

Gao, S., Wan, Y., Zheng, G., Luo, K., Kannan, K., Giesy, J.P., Lam, M.H.W.W., Hu, J., 2015. Organobromine compound profiling in human adipose: Assessment of sources of bromophenol. Environ. Pollut. 204, 81–89.

Greaves, A.K., Su, G., Letcher, R.J., 2016. Environmentally relevant organophosphate triesters in herring gulls: In vitro biotransformation and kinetics and diester metabolite formation using a hepatic microsomal assay. Toxicol. Appl. Pharmacol. 308, 59–65.

Guo, J., Stubbings, W.A., Romanak, K., Nguyen, L.V., Jantunen, L., Melymuk, L., Arrandale, V., Diamond, M.L., Venier, M., 2018. Alternative flame retardant, 2,4,6-tris(2,4,6-tribromophenoxy)-1,3,5-triazine, in an E-waste recycling facility and house dust in North America. Environ. Sci. Technol. 52, 3599–3607.

Hakk, H., Letcher, R.J., 2003. Metabolism in the toxicokinetics and fate of brominated flame retardants—a review. Environ. Int. 29, 801–828.

Hamers, T., Kamstra, J.H., Sonneveld, E., Murk, A.J., Kester, M.H.A., Andersson, P.L., Legler, J., Brouwer, A., 2006. In vitro profiling of the endocrine-disrupting potency of brominated flame retardants. Toxicol. Sci. 92, 157–173.

Hammel, S.C., Phillips, A.L., Hoffman, K., Stapleton, H.M., 2018. Evaluating the use of silicone wristbands to measure personal exposure to brominated flame retardants. Environ. Sci. Technol. 52, 11875–11885.

Hassenklöver, T., Predehl, S., Pilli, J., Ledwolorz, J., Assmann, M., Bickmeyer, U., 2006. Bromophenols, both present in marine organisms and in industrial flame retardants, disturb cellular Ca2+ signaling in neuroendocrine cells (PC12). Aquat. Toxicol. 76, 37–45.

Ho, K.-L., Yau, M.-S., Murphy, M.B., Wan, Y., Fong, B.M.W., Tam, S., Giesy, J.P., Leung, K.S.Y., Lam, M.H.W., 2015. Urinary bromophenol glucuronide and sulfate conjugates: Potential human exposure molecular markers for polybrominated diphenyl ethers. Chemosphere 133, 6–12.

Hou, X., Yu, M., Liu, A., Li, Y., Ruan, T., Liu, J., Schnoor, J.L., Jiang, G., 2018. Biotransformation of tetrabromobisphenol A dimethyl ether back to tetrabromobisphenol A in whole pumpkin plants. Environ. Pollut. 241, 331–338.

Koch, C., Sures, B., 2018. Environmental concentrations and toxicology of 2,4,6-tribromophenol (TBP). Environ. Pollut. 233, 706–713.

Leiker, T.J., Abney, S.R., Goodbred, S.L., Rosen, M.R., 2009. Identification of methyl triclosan and halogenated analogues in male common carp (*Cyprinus carpio*) from Las Vegas Bay and semipermeable membrane devices from Las Vegas Wash. Nevada. Sci. Total Environ. 407, 2102–2114.

Leonetti, C., Butt, C.M., Hoffman, K., Hammel, S.C., Miranda, M.L., Stapleton, H.M., 2016a. Brominated flame retardants in placental tissues: associations with infant sex and thyroid hormone endpoints. Environ. Health 15, 113.

Leonetti, C., Butt, C.M., Hoffman, K., Miranda, M.L., Stapleton, H.M., 2016b. Concentrations of polybrominated diphenyl ethers (PBDEs) and 2,4,6-tribromophenol in human placental tissues. Environ. Int. 88, 23–29.

Leonetti, C.P., Butt, C.M., Stapleton, H.M., 2018. Disruption of thyroid hormone sulfotransferase activity by brominated flame retardant chemicals in the human choriocarcinoma placenta cell line, BeWo. Chemosphere 197, 81–88.

Li, X., Qiu, S., Shi, J., Wang, S., Wang, M., Xu, Y., Nie, Z., Liu, C., Liu, C., 2019. A new function of copper zinc superoxide dismutase: as a regulatory DNA-binding protein in gene expression in response to intracellular hydrogen peroxide. Nucleic Acids Res. 47, 5074–5085.

Livak, K.J., Schmittgen, T.D., 2001. Analysis of relative gene expression data using real-time quantitative PCR and the 2−ΔΔCT method. Methods 25, 402–408.

Lörchner, D., Kraus, W., Köppen, R., 2019. Photodegradation of the novel brominated flame retardant 2,4,6-tris-(2,4,6-tribromophenoxy)-1,3,5-triazine in solvent system: Kinetics, photolysis products and pathway. Chemosphere 229, 77–85.

Lörchner, D., Kroh, L.W., Köppen, R., 2018. First insights into electrochemical transformations of two triazine-based brominated flame retardants in model systems. Analytical Methods 10, 5164–5170.

Luo, K., Gao, Q., Hu, J., 2019. Determination of 3-hydroxybenzo[a]pyrene glucuronide/sulfate conjugates in human urine and their association with 8-hydroxydeoxyguanosine. Chem. Res. Toxicol. 32, 1367–1373.

Luo, X.-Y., Takahara, T., Kawai, K., Fujino, M., Sugiyama, T., Tsuneyama, K., Tsukada, K., Nakae, S., Zhong, L., Li, X.-K., 2013. IFN-γ deficiency attenuates hepatic inflammation and fibrosis in a steatohepatitis model induced by a methionine- and choline-deficient high-fat diet. Am. J. Physiol. Gastrointest. Liver Physiol. 305, G891–G899.

Lupton, S.J., McGarrigle, B.P., Olson, J.R., Wood, T.D., Aga, D.S., 2009. Human liver microsome-mediated metabolism of brominated diphenyl ethers 47, 99, and 153 and identification of their major metabolites. Chem. Res. Toxicol. 22, 1802–1809.
Lyubimov, A.V., Babin, V.V., Kartashov, A.I., 1998. Developmental neurotoxicity and immunotoxicity of 2,4,6-tribromophenol in Wistar rats. Neurotoxicology 19, 303–312.
Matsubara, T., Katayama, K., Matsuoka, T., Fujiwara, M., Koga, M., Furukawa, S., 1999. Decreased interferon-gamma (IFN-gamma)-producing T cells in patients with acute Kawasaki disease. Clin. Exp. Immunol. 116, 554–557.
Monostory, K., Pascussi, J.-M., Kóbori, L., Dvorak, Z., 2009. Hormonal regulation of CYP1A expression. Drug Metab. Rev. 41, 547–572.
Mörck, A., Hakk, H., Örn, U., Wehler, E.K., 2003. Decabromodiphenyl ether in the rat: Absorption, distribution, metabolism, and excretion. Drug Metab. Dispos. 31, 900.
Norman Haldén, A., Nyholm, J.R., Andersson, P.L., Holbech, H., Norrgren, L., 2010. Oral exposure of adult zebrafish (Danio rerio) to 2,4,6-tribromophenol affects reproduction. Aquat. Toxicol. 100, 30–37.
Qiu, X., Bigsby, R.M., Hites, R.A., 2009. Hydroxylated metabolites of polybrominated diphenyl ethers in human blood samples from the United States. Environ. Health Perspect. 117, 93–98.
Qiu, X., Mercado-Feliciano, M., Bigsby, R., Hites, R., 2007. Measurement of polybrominated diphenyl ethers and metabolites in mouse plasma after exposure to a commercial pentabromodiphenyl ether mixture. Environ. Health Perspect. 115, 1052–1058.
Sandholm, A., Emanuelsson, B.M., Wehler, E.K., 2003. Bioavailability and half-life of decabromodiphenyl ether (BDE-209) in rat. Xenobiotica 33, 1149–1158.
Schreder, E., Uding, N.. Toxic TV binge, An investigation into flame retardants in televisions. Available at: https://saferchemicals.org/wp-content/uploads/2019/10/toxic_tv_binge_october_2019.pdf (Accessed March 9, 2021).
Stapleton, H.M., Letcher, R.J., Baker, J.E., 2004. Debromination of polybrominated diphenyl ether congeners BDE 99 and BDE 183 in the intestinal tract of the common carp (*Cyprinus carpio*). Environ. Sci. Technol. 38, 1054–1061.
Stapleton, H.M., Kelly, S.M., Pei, R., Letcher, R.J., Gunsch, C., 2008. Metabolism of polybrominated diphenyl ethers (PBDEs) by human hepatocytes in vitro. Environ. Health Perspect. 117, 197–202.
Stubbings, W.A., Nguyen, L.V., Romanak, K., Jantunen, L., Melymuk, L., Arrandale, V., Diamond, M.L., Venier, M., 2019. Flame retardants and plasticizers in a Canadian waste electrical and electronic equipment (WEEE) dismantling facility. Sci. Total Environ. 675, 594–603.
Su, G., Letcher, R.J., Crump, D., Farmahin, R., Giesy, J.P., Kennedy, S.W., 2014. Photolytic degradation products of two highly brominated flame retardants cause cytotoxicity and mRNA expression alterations in chicken embryonic hepatocytes. Environ. Sci. Technol. 48, 12039–12046.
Su, G., Letcher, R.J., Crump, D., Farmahin, R., Giesy, J.P., Kennedy, S.W., 2016. Sunlight irradiation of highly brominated polyphenyl ethers generates polybenzofuran products that alter dioxin-responsive mRNA expression in chicken hepatocytes. Environ. Sci. Technol. 50, 2318–2327.
Su, G., Letcher, R.J., Farmahin, R., Crump, D., 2018. Photolysis of highly brominated flame retardants leads to time-dependent dioxin-responsive mRNA expression in chicken embryonic hepatocytes. Chemosphere 194, 352–359.
Sun, J., Liu, J., Yu, M., Wang, C., Sun, Y., Zhang, A., Wang, T., Lei, Z., Jiang, G., 2013. In vivo metabolism of 2,2′,4,4′-tetrabromodiphenyl ether (BDE-47) in young whole pumpkin plant. Environ. Sci. Technol. 47, 3701–3707.
Sun, J., Pan, L., Su, Z., Zhan, Y., Zhu, L., 2016. Interconversion between methoxylated and hydroxylated polychlorinated biphenyls in rice plants: An important but overlooked metabolic pathway. Environ. Sci. Technol. 50, 3668–3675.
Takigami, H., Suzuki, G., Hirai, Y., Sakai, S.-I., 2009. Brominated flame retardants and other polyhalogenated compounds in indoor air and dust from two houses in Japan. Chemosphere 76, 270–277.
Wang, F., Wang, S., Yang, K., Liu, Y.-Z., Yang, K., Chen, Y., Fang, Z.-Z., 2020. Inhibition of UDP-glucuronosyltransferases (UGTs) by bromophenols (BPs). Chemosphere 238, 124645.
Wang, H.-S., Du, J., Ho, K.-L., Leung, H.-M., Lam, M.-H.-W., Giesy, J.P., Wong, C.-K.-C., Wong, M.-H., 2011. Exposure of Hong Kong residents to PBDEs and their structural analogues through market fish consumption. J. Hazard. Mater. 192, 374–380.
Xiong, P., Yan, X., Zhu, Q., Qu, G., Shi, J., Liao, C., Jiang, G., 2019. A review of environmental occurrence, fate, and toxicity of novel brominated flame retardants. Environ. Sci. Technol. 53, 13551–13569.
Yamada, T., Ozaki, N., Kato, Y., Miura, Y., Oiso, Y., 2006. Insulin downregulates angiopoietin-like protein 4 mRNA in 3T3-L1 adipocytes. Biochem. Biophys. Res. Commun. 347, 1138–1144.
Zalko, D., Prouillac, C., Riu, A., Perdu, E., Dolo, L., Jouanin, I., Canlet, C., Debrauwer, L., Cravedi, J.P., 2006. Biotransformation of the flame retardant tetrabromo-bisphenol A by human and rat sub-cellular liver fractions. Chemosphere 64, 318–327.
Zhang, P., Meng, L., Song, L., Du, J., Du, S., Cui, W., Liu, C., Li, F., 2018. Roles of perilipins in diseases and cancers. Curr. Genomics 19, 247–257.
Zhang, Q., Liu, Y., Lin, Y., Kong, W., Zhao, X., Ruan, T., Liu, J., Schnoor, J.L., Jiang, G., 2019. Multiple metabolic pathways of 2,4,6-tribromophenol in rice plants. Environ. Sci. Technol. Lett. 53, 7473–7482.
Zhang, Y.-N., Chen, J., Xie, Q., Li, Y., Zhou, C., 2016. Photochemical transformation of five novel brominated flame retardants: Kinetics and photoproducts. Chemosphere 150, 453–460.
Zhang, Y., Strehin, I., Bedelbaeva, K., Gourevitch, D., Clark, L., Leferovich, J., Messersmith, P.B., Heber-Katz, E., 2015. Drug-induced regeneration in adult mice. Sci. Transl. Med. 7, 290ra292.
Zuiderveen, E.A.R., Slootweg, J.C., de Boer, J., 2020. Novel brominated flame retardants - A review of their occurrence in indoor air, dust, consumer goods and food. Chemosphere 255, 126816.